Crystallographic Study of the EptC Phosphoethanolamine Transferase Required for Polymyxin Resistance and Motility in *Campylobacter jejuni*

Authors

Christopher D. Fage[a]*, Dusty B. Brown[b]*, Joseph M. Boll[b], Adrian T. Keatinge-Clay[a] and M. Stephen Trent[b]

[a]Molecular Biosciences, University of Texas at Austin, 1 University Station, Stop A5300, Austin, Texas, 78712, United States

[b]Molecular Biosciences, University of Texas at Austin, 2506 Speedway, Stop A5000, Austin, Texas, 78712, United States

*These authors contributed equally to the preparation of this manuscript.

Correspondence email: adriankc@utexas.edu; strent@austin.utexas.edu

Supporting information

Figure S1. Negative F_o-F_c electron density maps reveal radiation damage to the Zn remote-wavelength dataset. Density (red mesh) for phospho-T266, Zn^{2+}, and disulfides (C262-C272, C312-C316, and C377-C385) of chain A from (*a*) Zn remote-wavelength and (*b*) Zn K-edge datasets, contoured at -3σ. These images are representative of the entire asymmetric unit of each dataset. Because the Zn K-edge dataset is of higher quality in these crucial regions, it was selected for deposition over the Zn remote-wavelength dataset.

Figure S2. Expression and isolation of cEptC proteins. *(a)* Mass spectrum of native cEptC protein used in crystallization experiments (u, atomic mass unit). *(b)* Mass spectrum of selenomethionine-derived cEptC protein used to obtain phases. *(c)* Mass spectrum of the cEptC T266S mutant demonstrating the absence of phosphate modification. *(d)* Coomassie-stained SDS-PAGE gel showing the final purified cEptC protein; lane 1, molecular weight marker; lane 2, cell-free lysate of *E. coli* cells expressing cEptC; lane 3, purified cEptC protein. *(e)* Representative native cEptC protein crystals used in X-ray diffraction experiments.

Figure S3. Topology map of cEptC. α-Helices (green cylinders) are labeled α1 to α11 and β-strands (red arrows) are labeled β1 to β8, beginning from the N-terminus, as in Figure 2. The position of the nucleophilic Thr266 on the N-terminus of α2 is indicated with a star. This image is adapted from the topology map generated by uploading the cEptC coordinate file to the PDBsum server (Laskowski, 2009).

Figure S4. Surface rendition of *(a)* cEptC, compared with *(b)* cLptA (PDB 4KAY) and *(c) B. subtilis* cLtaS (PDB 2W8D). In the lower panel, each image is rotated 90^{o} to the left. Phosphothreonine residues, represented as spheres, indicate the locations of the active sites. Yellow regions are unique to cLptA and blue regions are unique to cLtaS, as in Fig. 3.

Figure S5. Phosphothreonine is located on the N-terminal end of the nucleophilic helix (α2). A helical dipole and neighboring Zn^{2+} (not shown) stabilize the deprotonated side chain of T266, activating the residue as a nucleophile capable of generating a phospho-intermediate. F_o-F_c omit map density for phosphothreonine (green mesh) is contoured to 4.0σ.

Figure S6. Minimized sequence alignment (Clustal Omega (Sievers & Higgins, 2014)) of representative phospho-form transferases in the COG2194 and COG1368 groups, demonstrating conservation of active-site residues. COG2194 consists of putative membrane-associated, metal-dependent hydrolases, including pEtN transferases such as EptC and LptA; COG1368 includes phosphoglycerol and related transferases of the alkaline phosphatase superfamily, such as LtaS. EptC and LtaS residues are labeled under alignments for COG2194 and COG1368, respectively. The locus tags used in the sequence alignments are as follows: Ng Lpt6 (*Neisseria gonorrhoea,* NGO2071), Ng PptA (*N. gonorrhoea,* NGO1540), Nm Lpt3 (*N. meningitidis,* NMB2010), Ec CptA (*E. coli,* b3955), Ec EptB (*E. coli,* Y75_p3631), Hp EptA (*Helicobacter pylori,* HP0022), Ab EptA (*Acinetobacter baumannii,* ABAYE0731), Nm LptA (*N. meningitidis* NMB1638), Ec EptA (*E. coli,* Y75_p4001), Kp

A79E_3434 (*Klebsiella pneumonia,* A79E_3434), Ws WS0643 (*Wolinella succinogens,* WS0643), Cj EptC (*C. jejuni,* Cj0256), Hh HH0805 (*H. hepaticus,* HH0805), Ec MdoB (*E. coli,* Y75_p4244), Sa LtaS (*S. aureus,* MS7_0770), Nm PptB (*N. meningitidis,* NMV0885).

Figure S7. Metal-binding sites of *(a)* cEptC, *(b)* cLptA (PDB 4KAY), and *(c) B. subtilis* cLtaS (PDB 2W8D) are conserved. Anomalous difference density for Zn^{2+} (magenta mesh) of cEptC is contoured to 6σ. Coordination bonds between side chains and metal ions are indicated with dashed lines. *(d)* Superposed models between *a* and *b* (30 atoms, r.m.s.d. = 0.26 Å) and *a* and *c* (21 atoms, r.m.s.d. = 0.18 Å) are displayed as one image with the coordinates of *a* as a reference.

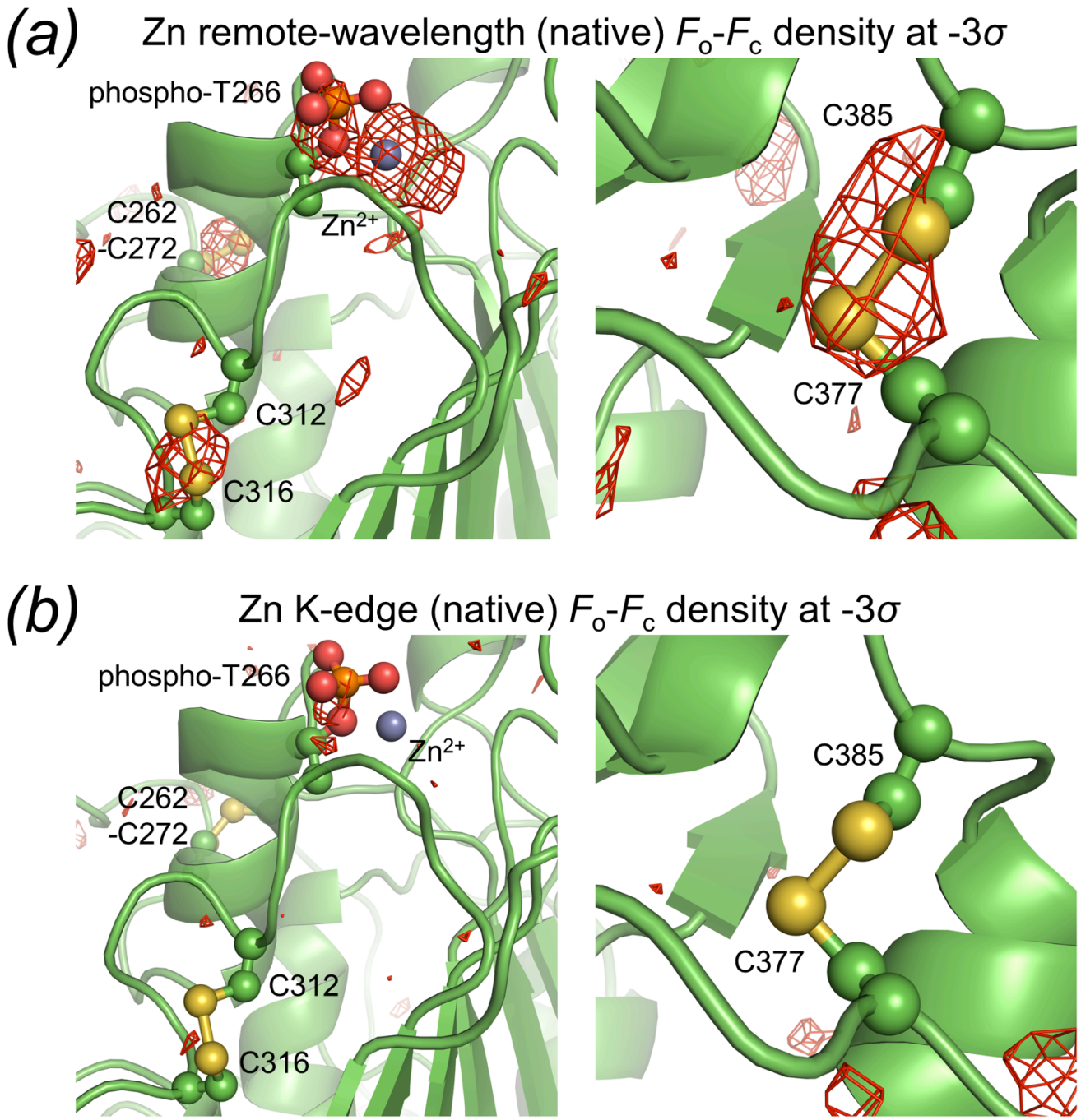
(a)
Zn remote-wavelength (native) F_o-F_c density at -3σ
phospho-T266
C262
-C272
Zn^{2+}
C312
C316
C385
C377
(b)
Zn K-edge (native) F_o-F_c density at -3σ
phospho-T266
Zn^{2+}
C262
-C272
C312
C316
C385
C377

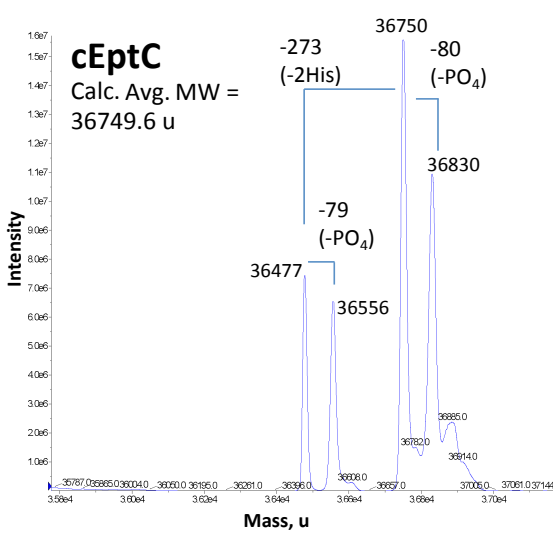
cEptC
Calc. Avg. MW =
36749.6 u
-273
(-2His)
-80
(-PO4)
-79
(-PO4)
36750
36830
36477
36556
Intensity
Mass, u

(a)

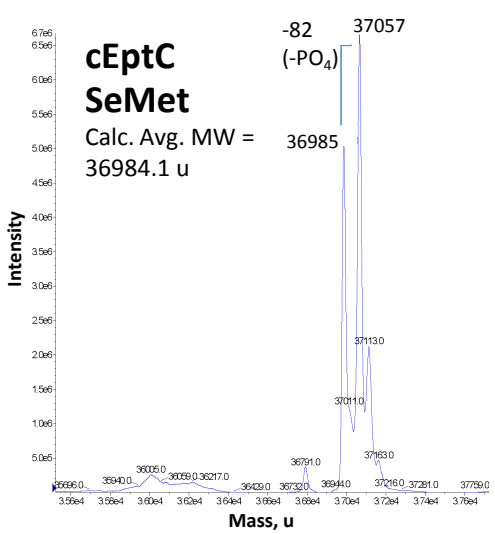
cEptC
SeMet
Calc. Avg. MW =
36984.1 u
-82
(-PO4)
37057
36985
Intensity
Mass, u

(b)

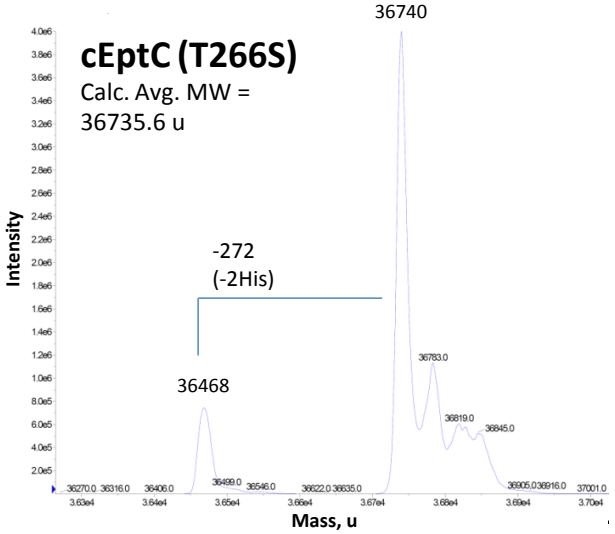
cEptC (T266S)
Calc. Avg. MW =
36735.6 u
36740
-272
(-2His)
36468
Intensity
Mass, u

(c)

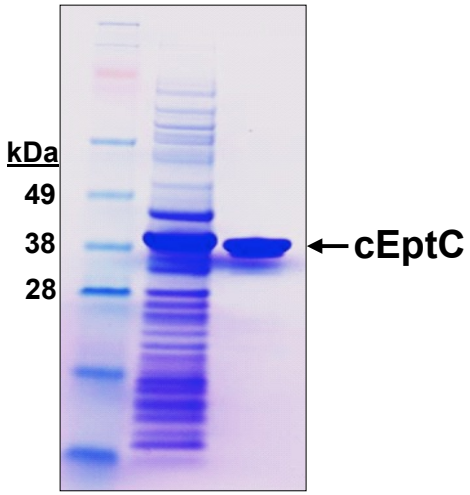
kDa
49
38
28
cEptC

(d)

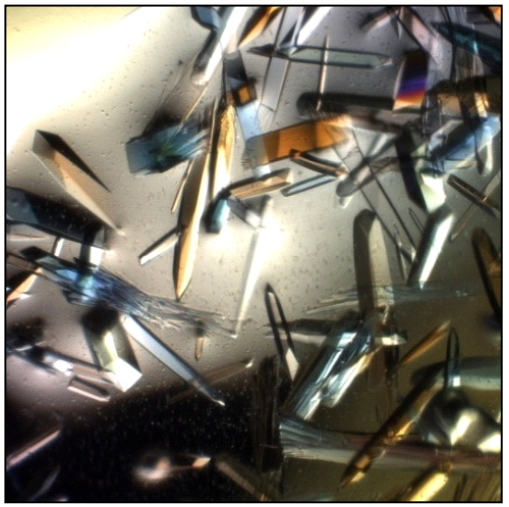

(e)

Fig S3

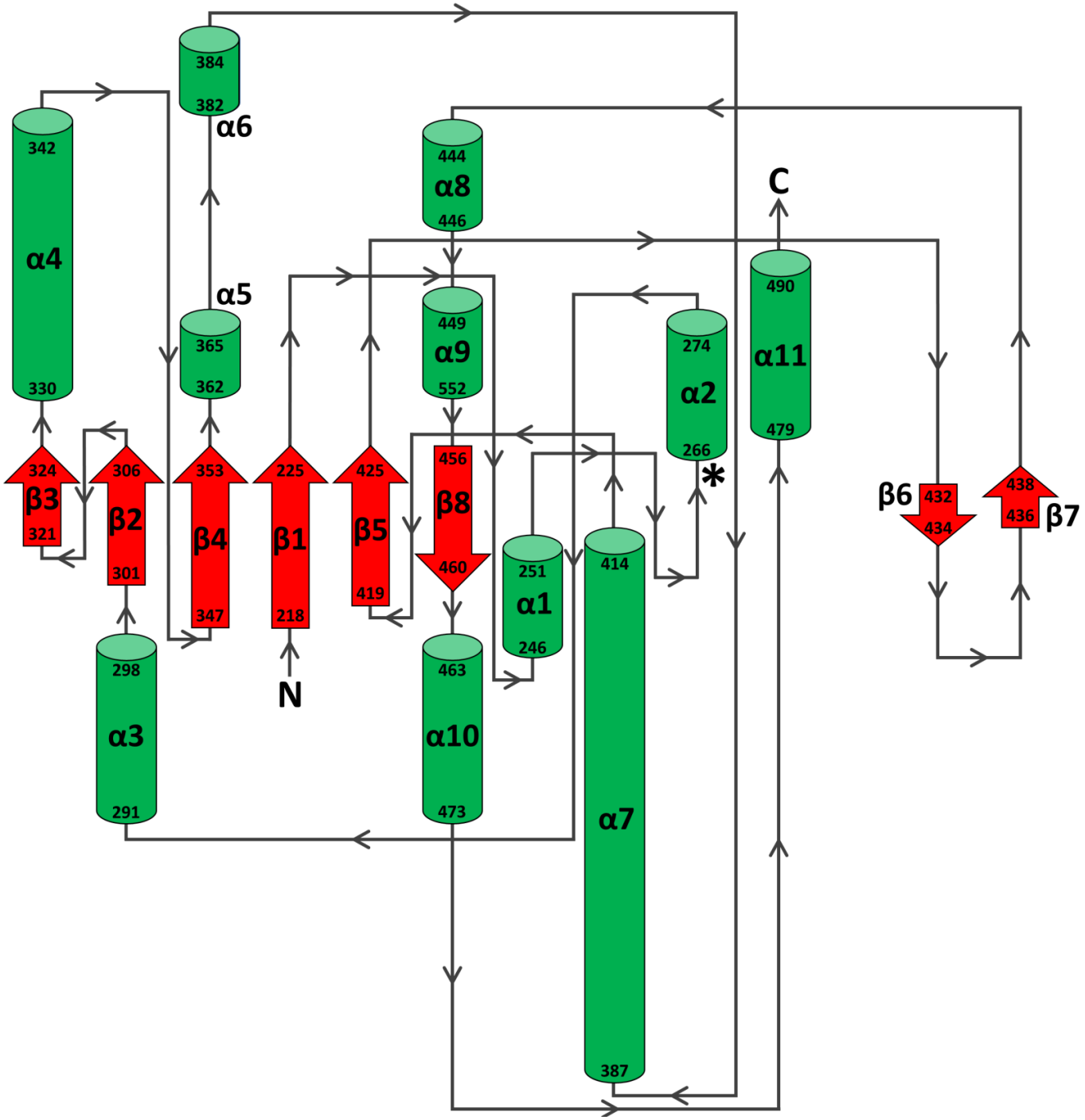
384
382
α6
342
α4
330
α5
365
362
444
α8
446
C
490
α11
479
449
α9
552
274
α2
266
*
324
β3
321
306
β2
301
353
β4
347
225
β1
218
N
425
β5
419
456
β8
460
251
α1
246
414
α7
387
β6
432
434
438
436
β7
298
α3
291
463
α10
473

Fig S4

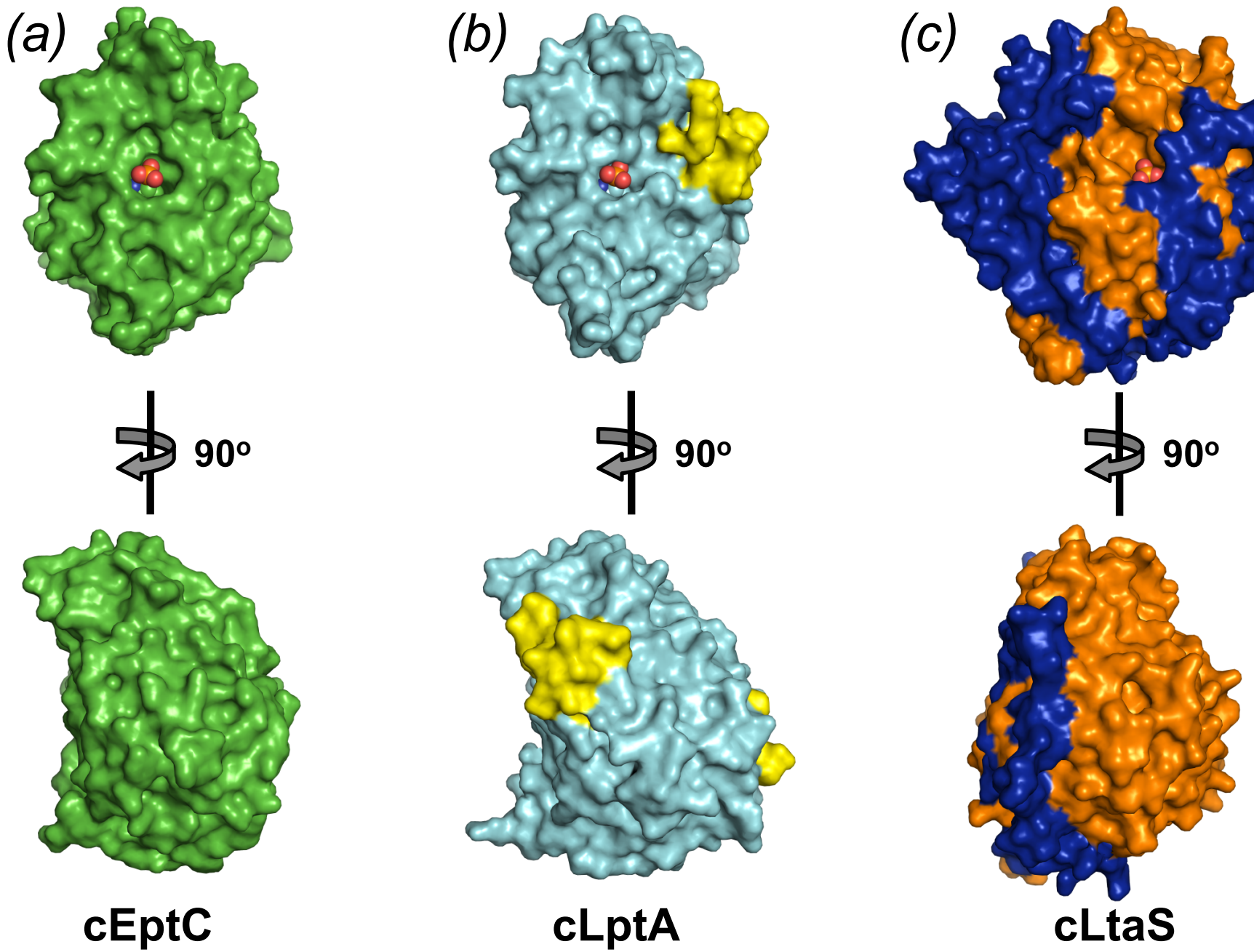

Fig S5

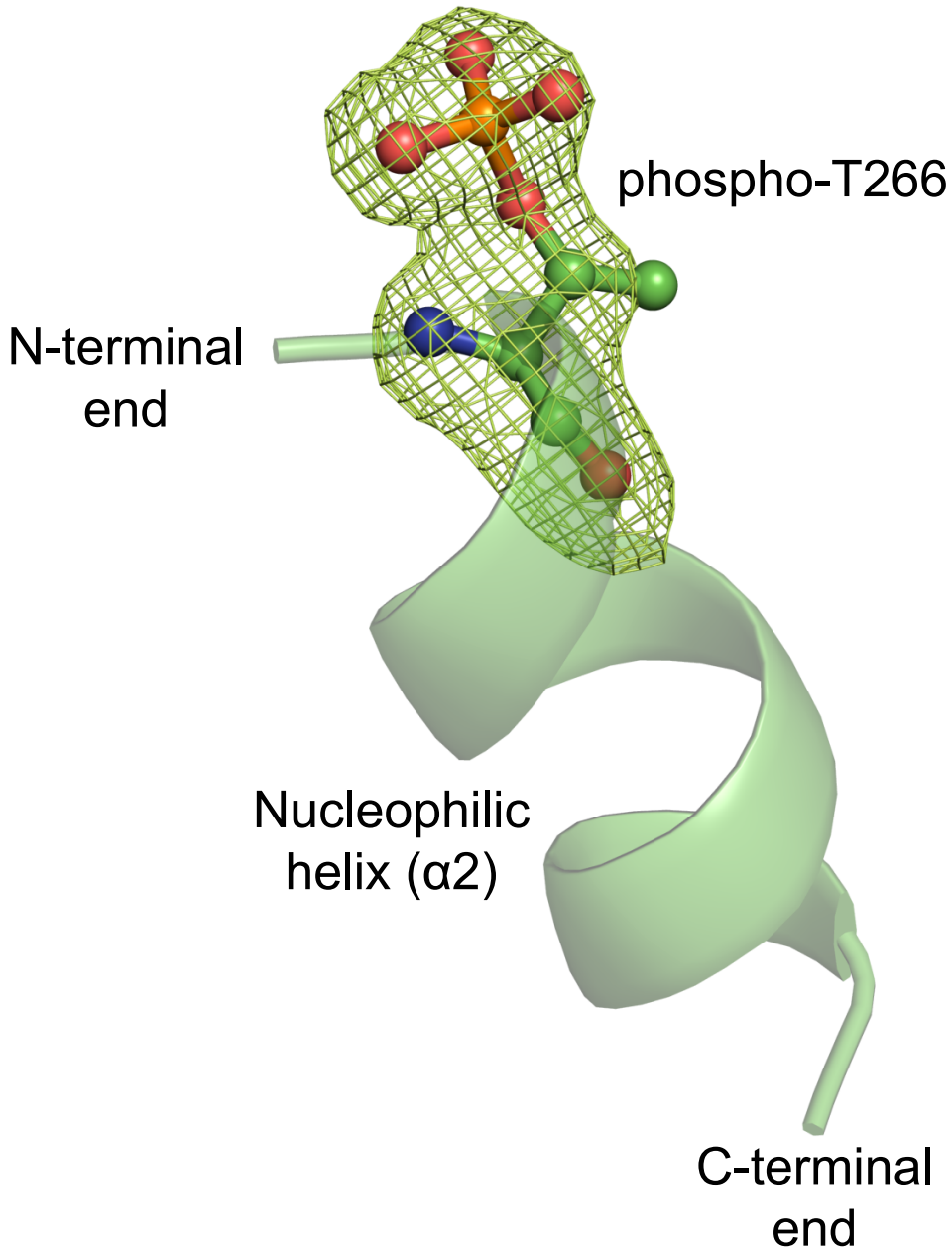
phospho-T266
N-terminal
end
Nucleophilic
helix (α2)
C-terminal
end

COG2194

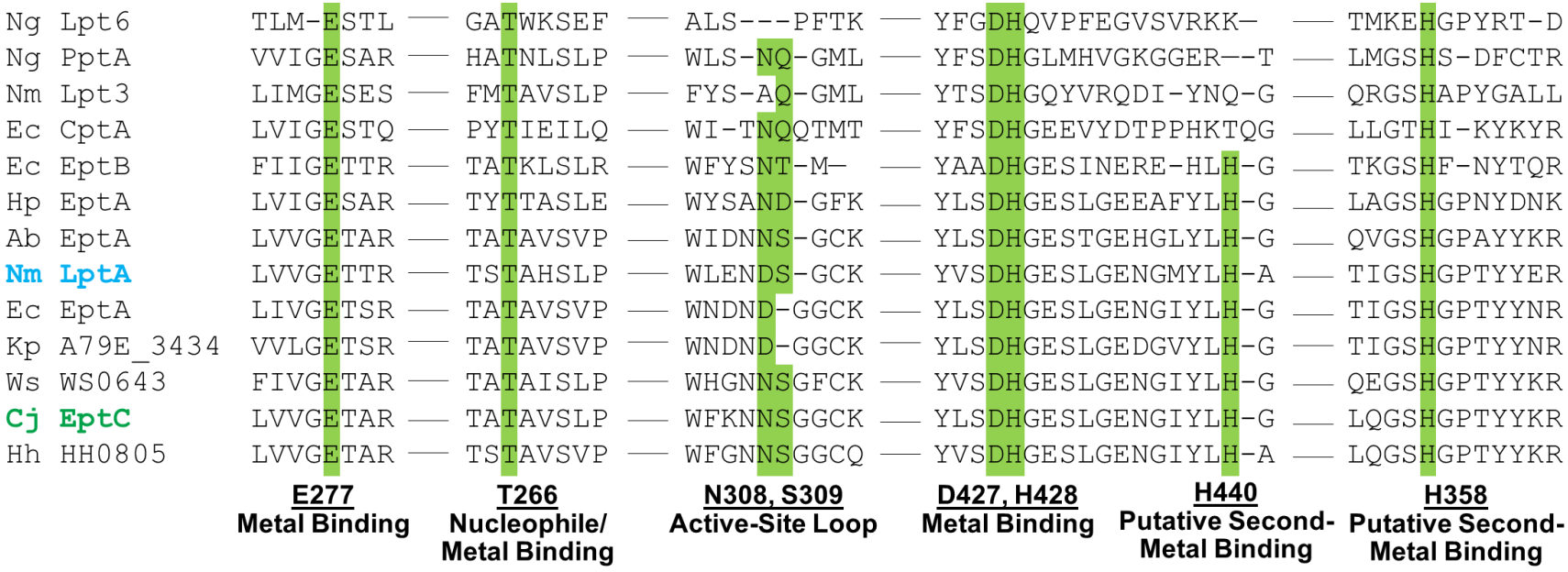

COG1368

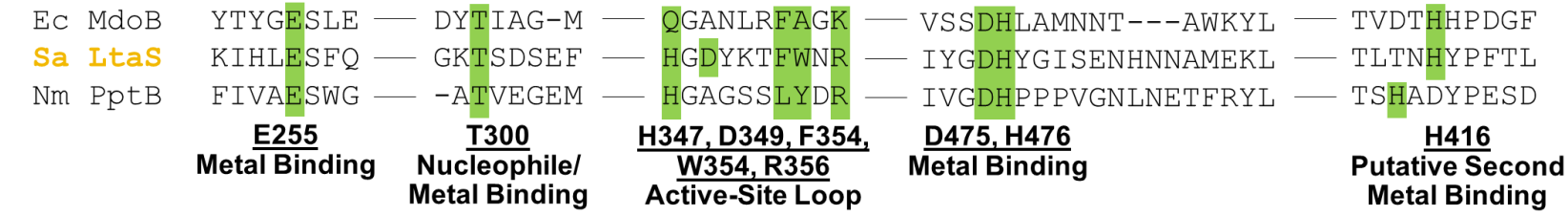

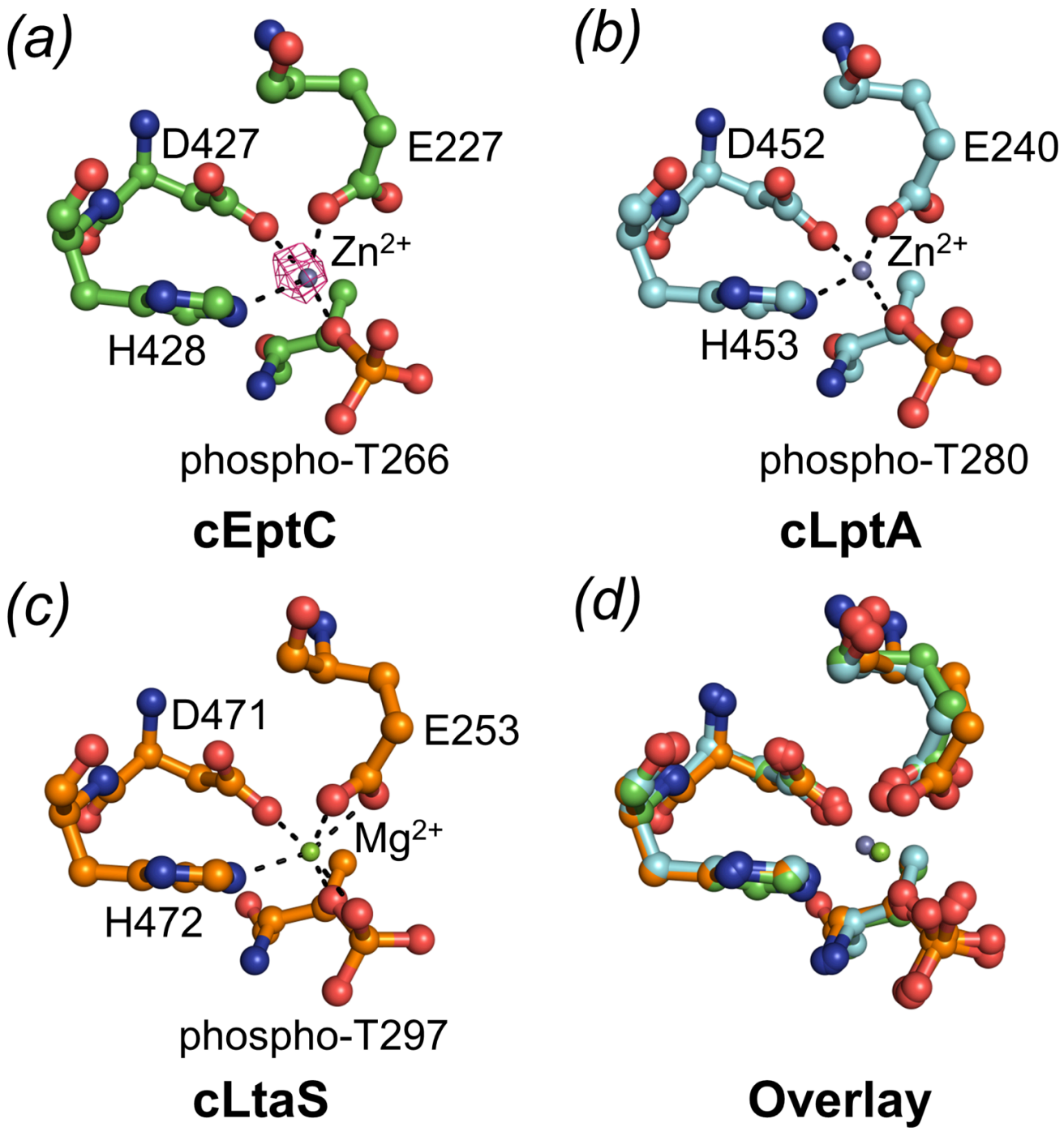
(a)
D427
E227
Zn2+
H428
phospho-T266
cEptC
(b)
D452
E240
Zn2+
H453
phospho-T280
cLptA
(c)
D471
E253
Mg2+
H472
phospho-T297
cLtaS
(d)
Overlay